

Electron-drift velocity determination in CF₄ and SF₆ in a strong electric field from breakdown curves of low-pressure RF discharge

V A Lisovskiy† and V D Yegorenkov‡

† Department of Physics and Technology, Kharkov State University, 4 Svobody Square, 310077, Kharkov, Ukraine

‡ Department of Physics, Kharkov State University, 4 Svobody Square, 310077, Kharkov, Ukraine

Received 25 May 1999

Abstract. In this paper we report the values of the electron-drift velocity in CF₄ and SF₆ within the range $E/p \approx 200\text{--}1000 \text{ V cm}^{-1} \text{ Torr}^{-1}$. We have used the recorded coordinates of the turning point on the breakdown curves of the rf capacitive discharge. We have also formulated the main requirements to the experimental device for correct recording of the breakdown curves of the low-pressure rf capacitive discharge. Our data are in good agreement with those of other authors who have used different approaches. We have also obtained the results on the electron-drift-velocity values within the E/p region where no other techniques are applicable. Our findings are also supported by numerical simulation data obtained with the application of a conventional Bolsig code.

1. Introduction

Carbon tetrafluoride (CF₄) and sulfur hexafluoride (SF₆) are widely used in plasma-assisted technology for processing semiconductor materials [1–3], in particle detectors [4, 5] and in gas-discharge switches of pulsed power [6, 7]. In order to improve the understanding of the processes occurring in such gas-discharge devices, one often applies numerical simulations. However, for CF₄ and SF₆ the calculations are impeded by the lack of data on the transport coefficients for electrons in these gases (especially for strong fields occurring in the cathode, near-electrode layers, strong double layers etc).

The electron-drift velocity V_{dr} characterizing the electric conductivity of a weakly ionized gas is one of the main parameters describing the transport of electrons in a gas under the action of the electrical field. A number of conventional techniques are used for measuring the electron-drift velocity (the time-of-flight technique, recording the optical emission of a moving electron swarm, the shutter technique etc). One may find, for example in [4–10] a detailed description of these techniques and the data on V_{dr} obtained with them. They enable one to determine the values of the electron-drift velocity within the range of relatively weak electrical fields $E/p \leq 100\text{--}200 \text{ V cm}^{-1} \text{ Torr}^{-1}$. For higher E/p values a self-sustained glow discharge may ignite between the electrodes of the experimental device and the V_{dr} measurements might become difficult to perform. Calculations for V_{dr} in CF₄ are also made only within the

range of weak fields E/p [11, 12]. The calculated V_{dr} values for SF₆ are obtained for higher E/p values (e.g. up to $E/p \leq 1000 \text{ V cm}^{-1} \text{ Torr}^{-1}$ in [13], but there is no satisfactory agreement between the V_{dr} values predicted in [13] and the experimental data.

In this paper the electron-drift velocity in CF₄ and SF₆ is determined from the recorded breakdown curves of the radio frequency (rf) capacitive low-pressure discharge. We have used the technique of determining V_{dr} , suggested in papers [14–16], and obtained the electron-drift-velocity values within the range $E/p \approx 200\text{--}1000 \text{ V cm}^{-1} \text{ Torr}^{-1}$. While for the techniques mentioned above the ignition of the self-sustained glow discharge is undesirable, the technique of determining the electron-drift velocity employed in our paper is based just on studying the electric breakdown of the gas.

2. Experimental device

The rf gas discharge was ignited in CF₄ and SF₆ within the pressure range $p = 10^{-2}\text{--}10 \text{ Torr}$ and at the rf field frequency $f = 13.56 \text{ MHz}$. The distance between the planar, round stainless-steel electrodes was changed within the limits $L = 8\text{--}29 \text{ mm}$. The electrodes were 100 mm in diameter. The rf voltage amplitude might vary within the range $U_{rf} = 0\text{--}1000 \text{ V}$.

The rf voltage was applied to one of the electrodes, whereas another one was grounded. A choke of 4 mH

inductance was connected across the electrodes to remove the dc bias.

We have not used any external ionization sources and we have studied exclusively the ignition of the self-sustained rf discharge.

We have applied the technique of recording rf breakdown curves as proposed earlier by Levitskii [17]. Near and to the right of the breakdown curve minimum we have fixed a certain value of the gas pressure in a discharge vessel and then slowly increased the rf voltage across the electrodes until the breakdown of the gas. Within the range of the multi-valued dependence of the rf breakdown voltage on the gas pressure (left-hand branch of the breakdown curve), we have fixed a certain value of the rf voltage at a sufficiently low pressure ($p \sim 10^{-3}$ – 10^{-2} Torr). Then we have increased the gas pressure inside the vessel until the occurrence of the gas breakdown. We have judged the point of breakdown, i.e. the ignition of the self-sustained RF discharge, by the appearance of light within the discharge vessel and the appearance of the active current in the electrode circuit.

The rf breakdown voltage U_{rf} was measured with ± 2 V accuracy within the range $U_{rf} \leq 500$ V and with ± 5 V accuracy within the range $U_{rf} > 500$ V. The breakdown time lag did not exceed 1–5 s within the ranges of gas pressure and applied rf voltages under study.

3. Experimental results

In order to determine the electron-drift velocity in CF_4 and SF_6 , we have used the coordinates of the turning point on the recorded breakdown curves of the capacitive rf discharge. This technique was suggested earlier in papers [14–16] and successfully applied for the determination of the electron-drift velocity in argon, hydrogen and air.

First we will consider the results of studying the breakdown of the rf discharge and the main requirements for the experimental device for correct recording of the breakdown curves of the rf discharge.

As is known [18–20], within the low-pressure range to the left of the breakdown-curve minimum of the rf discharge one observes the region of multi-valued dependence of the rf breakdown voltage U_{rf} on the gas pressure p . Figure 1 depicts several breakdown curves for the rf discharge in CF_4 . This figure also shows such a singular point as a turning point (at the pressure value $p = p_t$ and the rf voltage value $U_{rf} = U_t$). The existence of the turning point on the rf breakdown curve is associated with the following circumstances. At $p = p_t$ and $U_{rf} = U_t$, the amplitude of the electron displacement is approximately equal to one-half of the inter-electrode gap, thus leading to increased losses of electrons on the electrodes [16, 17]. This turning point is well expressed and the process of recording the rf-discharge breakdown curves in itself presents no particular difficulties.

However, as was shown earlier in [19], the shape of the recorded rf breakdown curves depends strongly on the way a rf generator is connected across the electrodes of the discharge vessel. Two schemes of such a connection exist. With one of them, a choke with an inductance of several mH is connected across the electrodes, thus removing a dc bias.

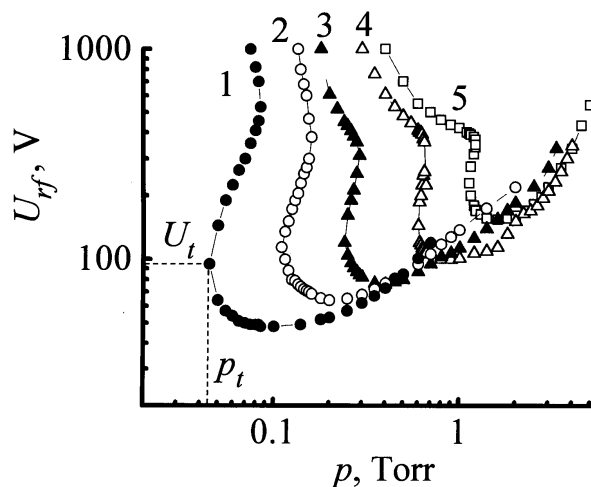


Figure 1. Breakdown curves of the rf discharge in CF_4 for different inter-electrode gaps. 1, $L = 29$ mm; 2, 20 mm; 3, 14 mm; 4, 10 mm; 5, 8 mm.

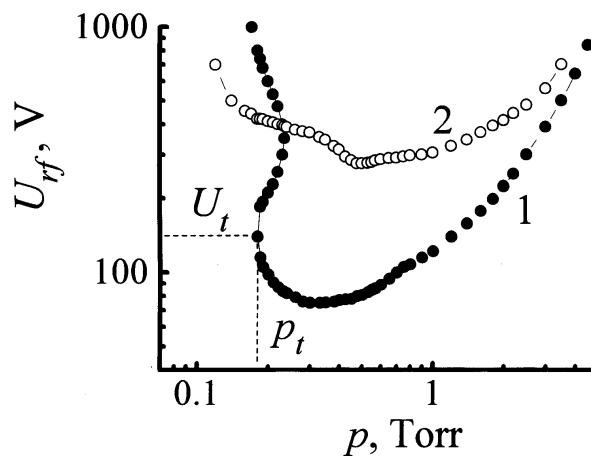


Figure 2. Breakdown curves of the rf discharge in CF_4 with (1) and without (2) the choke switched across the electrodes.

When the choke is absent, the dc voltage from the output stage of the rf generator charges the output circuit, the charge being distributed between the generator output and the electrodes of the vacuum vessel. Then it appears that beside the rf voltage a dc voltage is applied across the electrodes. Consequently, in the absence of the choke between the electrodes the gas breakdown occurs not in the rf field but in a combined (rf + dc) field. Figure 2 shows the breakdown curves of the rf discharge in CF_4 for the electrodes with the dc bias removed and present. One sees in figure 2 that, with the dc bias removed, the breakdown curve possesses the region of multi-valued dependence of the breakdown rf voltage on the gas pressure with a well expressed turning point. When the choke is absent, the multi-valued region may be absent and the curve itself lies in the range of higher rf voltages. A similar breakdown curve of the rf discharge may also be obtained when the electrodes of the experimental device possess different areas (e.g. a not very large rf electrode is placed in a metal vessel with grounded walls). Then a dc bias voltage appears across the electrodes. It is probable that such a situation occurred in [21].

Therefore, we present here the main requirements for the experimental device with which one can correctly record the breakdown curves of the rf discharge with the multi-valued region. The electrodes should be planar and parallel and they should have the same diameter, considerably exceeding the inter-electrode distance (1.5 to 2 times, at least). The walls of the discharge vessel should be made out of dielectric material (with the ideal case being two planar electrodes with the section of the glass tube vacuum-sealed between them). A choke must be connected across the electrodes to remove the dc bias voltage. The electric probes, substrate supports and other items must be removed from the discharge vessel because they introduce large distortions into the distribution of the vacuum rf field. There must be no magnetic ion vacuum pumps in the vacuum system of the experimental device because they may generate an undesirable steady magnetic field inside the discharge vessel. Only by meeting all these requirements is the correct recording of the breakdown curve of the rf capacitive discharge ensured.

Now let us describe briefly the technique of determining the electron-drift velocity from the breakdown curves of the rf discharge. A more detailed description of this technique was given in [17]. Consider the motion of electrons in a uniform rf field. The electron-drift velocity in the rf field (with $v_{en} \gg \omega$, where v_{en} is the frequency of electron-neutral collisions, $\omega = 2\pi f$ is the cyclic frequency of the rf field) may be written in the form

$$V(t) = \frac{eE_{rf}}{mv_{en}} \cos(\omega t) \quad (1)$$

where e and m are the electron charge and mass, respectively, and E_{rf} is the rf electric field amplitude. The amplitude value of the drift velocity $V_{dr} = eE_{rf}/mv_{en}$ is the maximum instantaneous velocity of electrons, corresponding to the maximum value (amplitude) of the rf field. Integrating (1) with respect to time, we obtain the amplitude of the electron displacement in the rf field:

$$A = \frac{eE_{rf}}{mv_{en}\omega} = \frac{V_{dr}}{\omega}. \quad (2)$$

On decreasing the gas pressure, the amplitude of the electron displacement increases and at the turning point of the rf breakdown curve at $p = p_t$ and $U_{rf} = U_t$ the condition $A \approx L/2$ holds. Thus, for the electron-drift velocity we have

$$V_{dr} = L\pi f. \quad (3)$$

For a fixed rf field frequency f and the inter-electrode gap L at the turning point of the breakdown curve the drift velocity V_{dr} is constant and it does not depend on the nature of the gas. The coordinates of the turning point enable one to calculate the ratio E/p , corresponding to the value of the electron-drift velocity obtained. For example, in figure 2 the coordinates of the first turning point are $p_t = 0.18$ Torr and $U_t = 140$ V; consequently, we obtain $E/p = U_t/p_t L \approx 432$ V cm⁻¹ Torr⁻¹. The value of the electron-drift velocity for the inter-electrode gap $L = 1.8$ cm is equal to $V_{dr} = 7.7 \times 10^7$ cm s⁻¹. For this point the absolute error in determining the pressure is not more than 0.005 Torr. The inter-electrode gap is measured

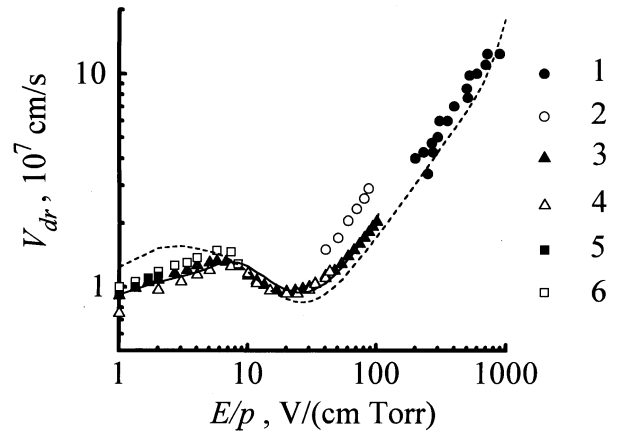


Figure 3. Electron-drift-velocity values in CF₄ against E/p obtained by different authors: 1, our data; 2, measured data given in [8]; 3, measured data given in [9]; 4, measured data given in [10]; 5, measured data given in [4]; 6, measured data given in [22]. The full curve is for simulation data given in [12]; and the dashed curve is for the data furnished with the Bolsig code.

to an accuracy of less than 0.2 mm. Thus the relative inaccuracy in determining the electron-drift velocity is within 5%.

Figure 3 shows the values of the electron-drift velocity in CF₄ obtained in this way. The same figure shows the measured and calculated V_{dr} values in CF₄, obtained in papers [4, 8–10, 12, 22]. To our knowledge there are no measured or calculated data from other authors on the V_{dr} values within the range $E/p > 200$ V cm⁻¹ Torr⁻¹. Therefore, we have performed the calculations of V_{dr} with the help of the Bolsig code (Kinema Research and Software) [23], which one may freely download from the server of this company. The drift-velocity values obtained with the Bolsig code within the range $E/p = 1$ – 1000 V cm⁻¹ Torr⁻¹ are shown in figure 3. For strong fields, which are of interest to us (to the left of the minimum of the function $V_{dr}(E/p)$), the Bolsig code predicts V_{dr} values which are approximately 1.2 times less than our data as well as the results of other authors. For $E/p \geq 500$ V cm⁻¹ Torr⁻¹ the Bolsig code ceases to find the steady value of the average electron energy. One observes a sharp increase of the calculated values of the electron-drift velocity; therefore, within this range of E/p the Bolsig code becomes inapplicable for calculating the parameters of electron motion in the strong electric fields. This disagreement is actually not surprising because in the Bolsig code the angular dependence of the velocity distribution function is expanded in Legendre polynomials and only the first two terms in this expansion are retained (so-called two-term expansion).

Figure 4 depicts the drift velocity values we have obtained in SF₆. The same figure also presents V_{dr} values in SF₆, measured in papers [24–28] and calculated in papers [13, 29–33], as well as those we have calculated with the Bolsig code. For $E/p \approx 200$ V cm⁻¹ Torr⁻¹ the V_{dr} values we have obtained for SF₆ are in good agreement with the measured data of other authors. Note that the Bolsig code describes the measured data for SF₆ satisfactorily within the total E/p range presented in figure 4. The V_{dr} values

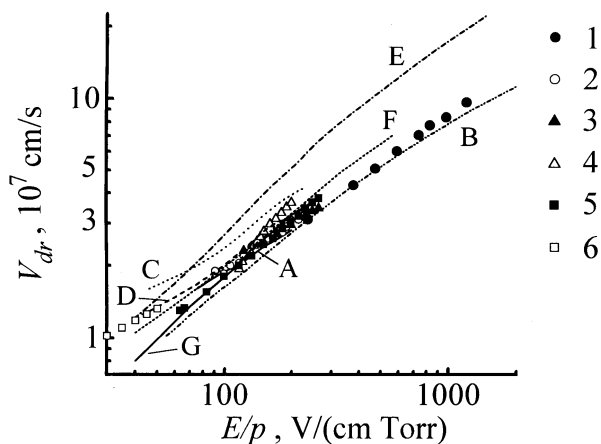


Figure 4. Electron-drift-velocity values in SF₆ against E/p obtained by different authors: 1, our data; 2, measured data given in [28]; 3, measured data given in [26]; 4, measured data given in [25]; 5, measured data given in [27]; 6, measured data given in [24]. Curve A is for the data calculated in [30], curve B is for the data furnished with the Bolsig code, curve C is for the data calculated in [33], curve D is for the data calculated in [32], curve E is for the data calculated in [13], curve F is for the data calculated in [29] and curve G is for the data calculated in [31].

predicted in paper [13] for large E/p values are 1.5 to 2 times higher than the measured ones, whereas the calculated V_{dr} values [30–33] are in a markedly better agreement with measured data.

4. Main conclusions

In this paper we have determined the values of the electron-drift velocity in CF₄ and SF₆ within the range $E/p \approx 200$ – $1000 \text{ V cm}^{-1} \text{ Torr}^{-1}$ accumulated in figures 3 and 4. In order to find the V_{dr} values, we have used the recorded coordinates of the turning point on the breakdown curves of the rf capacitive discharge. We have also formulated the main requirements for the experimental device for correct recording of the breakdown curves of the low-pressure rf capacitive discharge consisting, in part, in carefully removing the dc bias voltage across the electrodes of the discharge vessel. The data we have obtained with our technique are in good agreement with those of other authors who have used different approaches. Moreover, we have obtained the results for the electron-drift-velocity values within the E/p region where no other techniques are applicable. Our findings are also supported by numerical simulation data obtained with the application of a conventional code.

Acknowledgments

We wish to thank Dr L G Christophorou of the National Institute of Standards and Technology, Gaithersburg, Maryland, USA for supplying us with the excellent material on the properties of CF₄ and SF₆ and also Professor Y Nakamura of Keio University, Japan for information support.

References

- [1] Kushner M J 1982 *J. Appl. Phys.* **53** 2923
- [2] Moreau W M 1988 *Semiconductor Lithography: Principles, Practices, and Materials* (New York: Plenum)
- [3] Manos D M and Flamm D L 1989 *Plasma Etching* (Boston, MA: Academic)
- [4] Christophorou L G, McCorkle D L, Maxey D V and Carter J G 1979 *Nucl. Instrum. Methods* **163** 141
- [5] Christophorou L G, Datskos P G and Carter J G 1991 *Nucl. Instrum. Methods A* **309** 160
- [6] Hunter S R, Carter J G and Christophorou L G 1985 *J. Appl. Phys.* **58** 3001
- [7] Christophorou L G and Van Brunt R J 1995 *IEEE Trans. Dielectric Electrical Insul.* **2** 952
- [8] Naidu M S and Prasad A N 1972 *J. Phys. D: Appl. Phys.* **5** 983
- [9] Hunter S R, Carter J G and Christophorou L G 1988 *Phys. Rev. A* **38** 58
- [10] Christophorou L G, Olthoff J K and Rao M V V S 1996 *J. Phys. Chem. Ref. Data* **25** 1341
- [11] Curtis M G, Walker I C and Mathieson K J 1988 *J. Phys. D: Appl. Phys.* **21** 1271
- [12] Bordage M C, Segur P and Chouki A 1996 *J. Appl. Phys.* **80** 1325
- [13] Itoh H, Kawaguchi M, Satoh K, Miura Y, Nakao Y and Tagashira H 1990 *J. Phys. D: Appl. Phys.* **23** 299
- [14] Lisovskiy V A and Yegorenkov V D 1997 *Record-Abstracts of IEEE Int. Conf. on Plasma Science (San Diego, USA)* p 137
- [15] Lisovskiy V A 1998 *Tech. Phys. Lett.* **24** 308
- [16] Lisovskiy V A and Yegorenkov V D 1998 *J. Phys. D: Appl. Phys.* **31** 3349
- [17] Levitskii S M 1957 *Sov. Phys.-Tech. Phys.* **2** 887
- [18] Kropotov N Yu, Kachanov Yu A, Reuka A G, Lisovskiy V A, Yegorenkov V D and Farenik V I 1988 *Sov. Tech. Phys. Lett.* **14** 159
- [19] Kropotov N Yu, Lisovskiy V A, Kachanov Yu A, Yegorenkov V D and Farenik V I 1989 *Sov. Tech. Phys. Lett.* **15** 836
- [20] Lisovskiy V A and Yegorenkov V D 1994 *J. Phys. D: Appl. Phys.* **27** 2340
- [21] Smith H, Charles C and Boswell R 1998 *Proc. 4th Asia-Pacific Conf. on Plasma Science and Technology (Sydney, Australia)* p 105
- [22] Schmidt B and Polenz S 1988 *Nucl. Instrum. Methods Phys. Res. A* **273** 488
- [23] Pitchford L C, Boeuf J P and Morgan W L 1996 *Record-Abstracts of IEEE Int. Conf. on Plasma Science (Boston, USA)* p 154
- [24] Harris F M and Jones G J 1971 *J. Phys. B: At. Mol. Phys.* **4** 1536
- [25] Naidu M S and Prasad A N 1972 *J. Phys. D: Appl. Phys.* **5** 1090
- [26] Teich T H and Sangi B 1972 *Proc. Int. Symp. on High Voltage Technology (Munich: Plener)* p 391
- [27] Aschwanden T 1984 *Gaseous Dielectrics* vol IV, ed L G Christophorou and M O Pace (New York: Pergamon) p 24
- [28] Nakamura Y 1988 *J. Phys. D: Appl. Phys.* **21** 67
- [29] Kline L E, Davies D K, Chen C L and Chantray P J 1979 *J. Appl. Phys.* **50** 6789
- [30] Itoh H, Shimozuma M and Tagashira H 1980 *J. Phys. D: Appl. Phys.* **13** 1201
- [31] Novak J P and Frechette M F 1984 *J. Appl. Phys.* **55** 107
- [32] Itoh H, Miura Y, Ikuta N, Nakao Y and Tagashira H 1988 *J. Phys. D: Appl. Phys.* **21** 922
- [33] Satoh K, Itoh H, Nakao Y and Tagashira H 1988 *J. Phys. D: Appl. Phys.* **21** 931